HHS Public Access

Author manuscript

Eur Urol. Author manuscript; available in PMC 2017 July 19.

Published in final edited form as:

Eur Urol. 2017 January ; 71(1): 145–146. doi:10.1016/j.eururo.2016.06.019.

PSMA-Targeted ^{18}F-DCFPyL PET/CT Imaging of Clear Cell Renal Cell Carcinoma: Results from a Rapid Autopsy

Michael A. Gorin[a,*], **Steven P. Rowe**[b], **Jody E. Hooper**[c], **Max Kates**[a], **Hans-Joerg Hammers**[d], **Zsolt Szabo**[b], **Martin G. Pomper**[b], and **Mohamad E. Allaf**[a]

[a]The James Buchanan Brady Urological Institute and Department of Urology, Johns Hopkins University School of Medicine, Baltimore, MD, USA

[b]The Russell H. Morgan Department of Radiology and Radiological Science, Johns Hopkins University School of Medicine, Baltimore, MD, USA

[c]Department of Pathology, Johns Hopkins University School of Medicine, Baltimore, MD, USA

[d]Department of Medical Oncology, Sidney Kimmel Comprehensive Cancer Center, Johns Hopkins University School of Medicine, Baltimore, MD, USA

Prostate-specific membrane antigen (PSMA) is a type II transmembrane glycoprotein that is overexpressed by prostate cancer epithelial cells [1,2]. Despite the specificity implied by its name, PSMA is also expressed by endothelial cells within the neovasculature of a number of solid malignancies including clear cell renal cell carcinoma (ccRCC) [3–5]. Utilizing PSMA-targeted ^{18}F-DCFPyL positron emission tomography/computed tomography (PET/CT), we previously reported a sensitivity of 94.4% for detecting putative sites of disease in five patients with untreated metastatic ccRCC [6]. Notably, two (40%) of these patients had additional foci of radiotracer uptake (a total of 11 sites) that were suspicious for sites of metastases but lacked corresponding findings on conventional imaging. Similar results have since been reported using a gallium 68-labeled radiotracer targeting PSMA [7,8]. Combined, these data support a potential role for PSMA-targeted PET/CT to detect sites of otherwise clinically occult metastatic ccRCC. Available studies, however, have been limited by an inability to histologically sample PET-only detected lesions, leaving questions regarding the specificity of PSMA-targeted radiotracers for detecting true sites of disease. To address this, we imaged a patient with treatment-refractory ccRCC and, upon death, performed a rapid autopsy allowing for the histologic assessment of radiotracer-avid sites that were occult on conventional imaging.

The patient was a 52-yr-old man with metastatic ccRCC refractory to multiple lines of systemic therapy. Following failure to respond to immunotherapy with nivolumab, the patient elected for hospice care and was imaged with whole-body ^{18}F-DCFPyL PET/CT prior to death. Contemporaneously performed contrast-enhanced CT imaging of the chest,

*Corresponding author at: 600 North Wolfe Street, Marburg 134, Baltimore, MD 21287, USA. Tel.+1 410 502 7710; fax: +1 410 502 7711. mgorin1@jhmi.edu (M.A. Gorin).

Conflicts of interest: Martin G. Pomper is a coinventor on a US patent covering ^{18}F-DCFPyL and, as such, is entitled to a portion of any licensing fees and royalties generated by this technology. This arrangement has been reviewed and approved by the Johns Hopkins University in accordance with its conflict of interest policies. The remaining authors have nothing to disclose.

abdomen, and pelvis demonstrated 55 discrete sites of metastatic ccRCC. In total, 54 (98.1%) of these lesions had corresponding findings on PET/CT (Fig. 1). In addition, 12 sites of radiotracer uptake were observed that lacked findings on conventional imaging. Of these, eight (66.7%) were readily accessible at the time of rapid autopsy, including two (12.5%) lymph nodes, two (12.5%) muscular lesions, two (25%) cortical bone lesions, one (12.5%) dural lesion, and one (12.5%) bone marrow lesion. With the exception of a single bone lesion, the other seven sites (87.5%) were histologically confirmed to be metastatic ccRCC. All histologically proven sites of ccRCC were found to have PSMA expression localized to their neovasculature (Supplementary Fig. 1). Of note, the one false-positive bone lesion contained marked edema of the marrow space, suggesting the possibility of cancer that was missed due to sampling error (Supplementary Fig. 2). In addition, the one observed lesion on conventional imaging that was without corresponding radiotracer uptake was also sampled and found to be a necrotic lymph node with evidence of nonviable ccRCC (Supplementary Fig. 3).

In conclusion, data from this rapid autopsy support previous observations that PSMA-targeted PET/CT allows for the accurate detection of sites of metastatic ccRCC. Potential applications for this novel molecular imaging test include upfront staging of patients at risk for occult metastatic ccRCC and guidance of site-directed therapy (eg, surgical metastasectomy and stereotactic ablative radiotherapy) in patients with potentially curable oligometastatic disease. In addition, PSMA-targeted imaging may potentially be used to predict and/or assess response to systemic therapy. This is particularly relevant in ccRCC owing to the fact that PSMA is expressed in the neovasculature and many of the commonly used drugs for this disease target angiogenesis. An ongoing diagnostic trial (ClinicalTrials.gov identifier NCT02687139) aims to more precisely define the diagnostic accuracy of PSMA-targeted PET/CT across the various stages of ccRCC and to explore this novel imaging test in patients with non–clear cell variants of RCC.

Supplementary Material

Refer to Web version on PubMed Central for supplementary material.

Acknowledgments

Funding support: This study was funded by the National Institutes of Health (P30CA006973).

Appendix A. Supplementary data

Supplementary material related to this article can be found, in the online version, at http://dx.doi.org/10.1016/j.eururo.2016.06.019.

References

1. Ristau BT, O'Keefe DS, Bacich DJ. The prostate-specific membrane antigen: lessons and current clinical implications from 20 years of research. Urol Oncol. 2014; 32:272–9. [PubMed: 24321253]
2. Rowe, SP., Gorin, MA., Allaf, ME., et al. PET imaging of prostate-specific membrane antigen in prostate cancer: current state of the art and future challenges Prostate Cancer Prostatic Dis In press. http://dx.doi.org/10.1038/pcan.2016.13

3. Chang SS, Reuter VE, Heston WD, Bander NH, Grauer LS, Gaudin PB. Five different anti-prostate-specific membrane antigen (PSMA) antibodies confirm PSMA expression in tumor-associated neovasculature. Cancer Res. 1999; 59:3192–8. [PubMed: 10397265]

4. Chang SS, Reuter VE, Heston WD, Gaudin PB. Metastatic renal cell carcinoma neovasculature expresses prostate-specific membrane antigen. Urology. 2001; 57:801–5. [PubMed: 11306418]

5. Baccala A, Sercia L, Li J, Heston W, Zhou M. Expression of prostate-specific membrane antigen in tumor-associated neovasculature of renal neoplasms. Urology. 2007; 70:385–90. [PubMed: 17826525]

6. Rowe SP, Gorin MA, Hammers HJ, et al. Imaging of metastatic clear cell renal cell carcinoma with PSMA-targeted ^{18}F-DCFPyL PET/CT. Ann Nucl Med. 2015; 29:877–82. [PubMed: 26286635]

7. Sawicki, LM., Buchbender, C., Boos, J., et al. Diagnostic potential of PET/CT using a ^{68}Ga-labelled prostate-specific membrane antigen ligand in whole-body staging of renal cell carcinoma: initial experience. Eur J Nucl Med Mol Imaging. In press. http://dx.doi.org/10.1007/s00259-016-3360-2

8. Rhee H, Tham CM, Thomas P, et al. MP03-12 Staging advanced and metastatic clear cell renal cell carcinoma with 68-gallium PSMA PET for treatment planning [abstract]. J Urol. 2016; 195:e23.

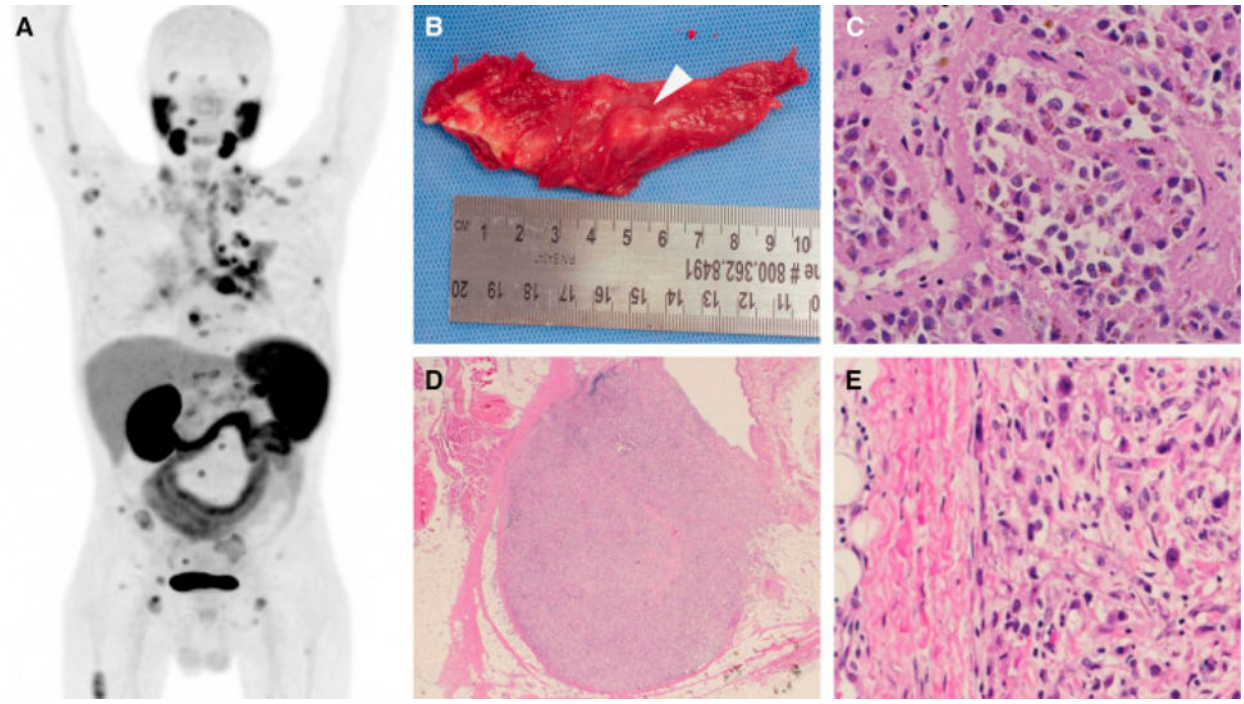

Fig. 1.

(a) Maximal intensity projection of the imaged patient. Normal biodistribution of the radiotracer includes the salivary glands, lacrimal glands, liver, spleen, kidneys, and small bowel. Excreted radiotracer is also observed in the ureters and bladder. All other sites of radiotracer uptake represent putative sites of metastatic clear cell renal cell carcinoma (ccRCC). (b) Gross image of a 10-mm nodule of ccRCC found within the right triceps muscle. This lesion was occult on conventional imaging and (c) histologically confirmed to be ccRCC (×200). (d) Low-power (×40) and (e) high-power (×200) images of a 6-mm intramammary lymph node with metastatic ccRCC observed only on ^{18}F-DCFPyL positron emission tomography/computed tomography.